Staggered field-induced tricritical behavior in the $S=\frac{1}{2}$ quasi-one-dimensional Ising antiferromagnet on a stacked triangular lattice: Monte Carlo simulations

E. Meloche and M. L. Plumer

*Department of Physics and Physical Oceanography, Memorial University of Newfoundland, St. John's,
Newfoundland A1B 3X7, Canada*

The impact of a staggered magnetic field due to quantum exchange mixing in the $S=\frac{1}{2}$ quasi-one-dimensional Ising antiferromagnet on a stacked triangular lattice is shown to induce a crossover from *XY* to tricritical universality at the phase transition to the partially disordered state. Using a unique combination of histogram and cluster heat-bath techniques, extensive Monte Carlo simulations are performed to explore the effects of a small applied field that emulates a previously proposed addition to the spin Hamiltonian formulated to account for unusual spin soliton excitations in such systems. It is argued that quantum fluctuations governing short-range order in low-dimensional frustrated spin systems generally can affect measured critical properties at the onset to long-range magnetic order. Our results explain recent high resolution neutron scattering data on $CsCoBr_3$.

PACS number(s): 75.40.Cx, 75.40.Mg, 75.45.+j, 05.10.Ln

I. INTRODUCTION

The recent emergence of exotic quantum spin order associated with the frustrated $S=\frac{1}{2}$ triangular antiferromagnet[1–5] follows decades of discovery of novel classical phase transitions in such systems.[6,7] Many frustrated spin systems also exhibit magnetic low dimensionality where dominant exchange interactions (J) are anisotropic, giving rise to quasi-one-dimensional (quasi-1D) or quasi-two-dimensional short-range order (SRO) at low temperatures. A consequence of both frustration and low-dimensional magnetic interactions is that the transition temperature to long-range order (LRO), T_N, is much reduced compared to its nominal value of $\sim J/K$. This allows for the possibility that fluctuation effects associated with well-developed SRO at temperatures above T_N can impact measured critical properties at the phase transition to LRO. Such effects can be particularly relevant in attempts to find meaningful comparisons between experimental and theoretical estimates of critical exponents which rely on results inaccessibly close to T_N. The present work demonstrates that quantum effects which govern low-dimensional spin dynamics can impact the effective critical properties of the three-dimensional (3D) system.

The Ising antiferromagnet on a stacked triangular lattice (ISTAF) with strong *c*-axis exchange and weak interchain exchange interactions is an example of such a model system. Strong quantum effects in $S=\frac{1}{2}$ $CsCoBr_3$ have recently been proposed to result in hidden chiral order associated with soliton dynamics.[8] Much earlier work demonstrated that exchange mixing due to an unquenched orbital moment and crystal field effects in the ISTAF give rise to an unusual contribution to the effective spin Hamiltonian in the form of a staggered magnetic field with a periodicity of 2 along the *c* axis. This term has been employed to explain low temperature inelastic neutron scattering from soliton excitations[9] in $CsCoCl_3$ and $CsCoBr_3$ and Raman data in $TlCoCl_3$.[10] Invoking such an effect relies on the well-developed SRO intrinsic to low-dimensional frustrated magnetic systems at low *T*. Examination of the impact of this field term on the measured

effective critical behavior observed close to T_N is important even though it may be strictly irrelevant in the renormalization group sense *at* T_N. In this work, the influence of this quantum staggered field in the $S=\frac{1}{2}$ quasi-1D ISTAF is emulated in Monte Carlo (MC) simulations by considering the influence of a small uniform magnetic field applied to a model with ferromagnetic intrachain interactions with antiferromagnetic (AF) interchain coupling. This type of effective quantum staggered field is not predicted to occur in the case of some other STAF's such as ($S=1$) $CsNiCl_3$ which has been shown to exhibit integer-spin Haldane-gap phenomena.[11]

Classical critical behavior in the ISTAF has been extensively investigated using numerous theoretical approaches, MC simulations, and experimentally. Despite the large number of studies, there is still no clear consensus in the literature regarding the critical exponents characterizing the phase transition between the partially disordered phase, where one of the three sublattices remains disordered, and the paramagnetic phase, at T_N. Most modeling results[6,12] support the notion from symmetry arguments that the transition at T_N belongs to the *XY* universality class.[13] There have been suggestions, however, from several MC simulations that critical exponents are close to mean-field tricritical,[14,15] but limited statistics and data analysis were used in these investigations. From the experimental standpoint, a number of past neutron scattering studies[6] of $CsCoBr_3$ and $CsCoCl_3$ have obtained sets of critical exponents that largely support the idea of *XY* critical behavior. Intriguingly, recent high resolution neutron scattering experiments on $CsCoBr_3$ by Mao *et al.*[16] revealed results which suggest tricritical mean-field behavior and it was speculated that this could be attributed to the anisotropic nature of the exchange interaction or a consequence of the quantum nature of the $S=\frac{1}{2}$ spins. Experimental data on weakly axial $S=1$ $CsNiCl_3$ with a quenched orbital moment[11] are consistent with *XY* universality.[6,17] Both types of experimental systems, strongly Ising and weakly Ising, exhibit magnetic transitions at T_N with the same symmetry and thus should belong to the same classical universality class.
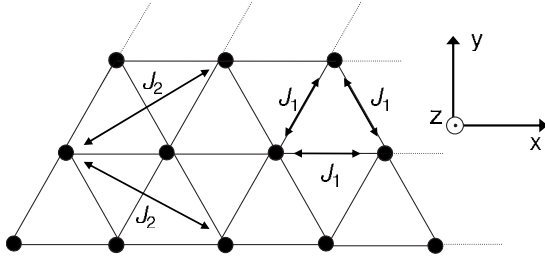
FIG. 1. Planar view of the stacked triangular lattice showing the nearest- and next-nearest-neighbor intralayer exchange interactions J_1 and J_2, respectively. The exchange coupling between interlayer neighbors is denoted by J_0 (not shown).

Motivated by the new experimental data of Mao *et al.*, extensive MC simulations using the efficient cluster heat bath (CHB) algorithm,[18,19] combined with the histogram method,[20] were used here to investigate the effects of anisotropic exchange as well as a small applied field on the critical properties of the classical ISTAF. This work serves to extend previous MC simulations of the ISTAF mentioned above, but especially that of Koseki and Matsubara,[15] where the CHB algorithm was used with strongly anisotropic exchange but with no applied field, as well as that of Netz and Berker[21] and Plumer and Mailhot[12] who considered *isotropic* exchange interactions with a nonzero applied field. The present results also complement MC simulations on the frustrated *XY*-STAF where anisotropy in the exchange interactions was shown to induce a first-order transition,[22] in agreement with recent experimental data.[23] An additional focus of our work is the careful analysis of the uncertainty associated with the procedure used to estimate critical exponents.

The MC simulation results discussed here are based on the order-parameter cumulant crossing method[24] used to estimate the critical temperature of the system. Finite-size scaling analysis at T_N was then used to extract estimates of the critical exponents μ, γ, and ν. Both of these techniques have been thoroughly tested on frustrated Ising and Heisenberg spin models.[24]

II. MODEL

For the purposes of determining classical critical behavior, it is adequate to use a model system with ferromagnetic exchange interactions along the c axis, J_0, with or without a small applied uniform field H directed along the c axis. A uniform magnetic field H acting on ferromagnetically aligned spins with $S_k^z = S$, where k is a layer index, is energetically equivalent ($E = -HS$) to a staggered field $H_{stag} = H(-1)^k$ acting on antiferromagnetically aligned spins with $S_k^z = S(-1)^k$. In addition to near-neighbor AF interactions between chains, J_1, the effects of a small next-nearest-neighbor exchange coupling, J_2, were also considered as in previous MC simulations.[26] A schematic illustration of the system is shown in Fig. 1. These effects can be incorporated in the Ising Hamiltonian:

$$\mathcal{H} = -\sum_{\langle i,j \rangle} J_{ij}\sigma_i\sigma_j - H\sum_i \sigma_i, \qquad (1)$$

where the spin at any site is $\sigma_i = \pm 1$. In zero applied field, four different cases were investigated with parameters listed

TABLE I. Exchange parameters used for the four zero-field cases.

Case	J_0	J_1	J_2
I	1.0	−1.0	0
II	10.0	−1.0	0
III	10.0	−1.0	0.1
IV	10.0	−0.3	0.001

in Table I. For all cases, J_0 and J_2 are ferromagnetic and J_1 is antiferromagnetic. Finite-size scaling analysis was also performed at five nonzero values of H for case II.

The isotropic case I ($|J_0| = |J_1|$) was previously investigated using the MC histogram method with periodic boundary conditions for an $N = L \times L \times L$ system.[12,25,26] Different sets of critical exponents characteristic of different universality classes were obtained in these previous studies, serving to illustrate the sensitivity of analyzing MC simulation data in frustrated systems. Cases II, III, and IV correspond to models with anisotropic quasi-1D exchange interactions (with $|J_0| \gg |J_1|$) for different values of J_2. The anisotropic case IV was previously investigated[18] using the CHB algorithm and estimates of the critical temperature and the critical exponents β and ν were obtained using a data collapse method.

The CHB algorithm employs open boundary conditions along the c axis and periodic boundary conditions in the other directions. For systems with quasi-1D exchange interactions, the CHB algorithm is more efficient than the Metropolis algorithm and allows for better statistics when simulating larger lattice sizes. We considered anisotropic lattices with $N = L \times L \times 10L$ and $L = 9, 12, \ldots, 33, 36$. These system sizes are smaller than those employed in Ref. 15. However, a significantly larger number of MC steps were used in any particular run. Averages were also performed over ten independent simulations using different random initial spin configurations. Estimates of the errors were obtained by taking the standard deviation from the different simulations. Runs of $1 \times 10^5 - 8 \times 10^5$ MC steps were used for equilibration, and $5 \times 10^5 - 1.2 \times 10^6$ MC steps were used to calculate averages of several thermodynamic quantities including the order parameter O, susceptibility χ_1, specific heat C, energy cumulant U_E, order-parameter cumulant U_M, and first logarithmic derivative of the order parameter V_1, as defined in Ref. 24. The primary order parameter O is defined in terms of the **Q**th Fourier component of the spin density as $O = |\sum_i \sigma_i \exp(i\mathbf{Q} \cdot \mathbf{R}_i)|/N$, with $\mathbf{Q} = (2\pi/3, 2\pi/3, 0)$ in units of the lattice constants associated with the simple hexagonal structure. In addition, the temperature dependence of the secondary order parameter O' with the wave vector $\mathbf{Q} = (0,0,0)$, corresponding to the uniform magnetization, was also examined. Relevance of this component of the spin density (in zero applied field) on the nature of the critical behavior in these systems has been previously speculated.[14,15]

Accurate estimation of the critical temperature is an essential first step in utilizing the histogram method for determining critical exponents. Temperature sweeps for the $L = 24$ system were initially performed using fewer MC steps to obtain a rough estimate of the transition temperature T_N by
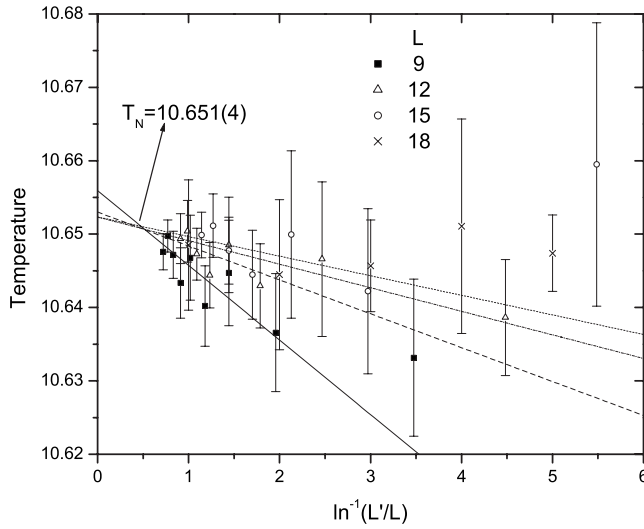
FIG. 2. Results of applying the order-parameter cumulant crossing method to estimate the critical temperature T_N for case II. The straight lines correspond to linear fits to the data with $\ln^{-1}(L'/L) \leqslant 2.2$.

locating the maxima of the susceptibility χ_1 and specific heat C. For example, for case IV, temperature scans from $T=6.8$ to 8.0 in increments of $\Delta T=0.05$ yielded an estimate of $T_N =7.40$. To determine the critical temperature more accurately, several histograms were generated at temperatures above and below T_N. In this case, histograms were generated at $T =7.34$, 7.36, 7.38, 7.40, and 7.42 for each lattice size L.

III. SIMULATION RESULTS AT ZERO FIELD

The order-parameter cumulant crossing method[27,28] was used for the sets of parameters of Table I at zero applied field. An illustrative example of the results for case II is presented in Fig. 2. For each case, we plot the temperature at
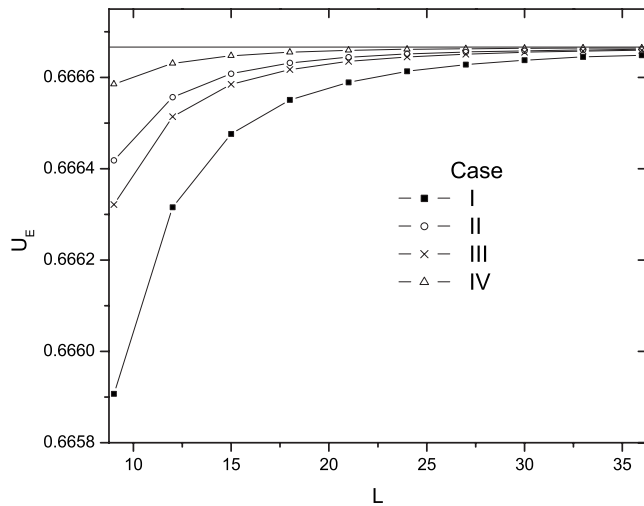

FIG. 3. Scaling of the energy cumulant U_E as a function of the lattice size L for the four zero-field cases. The horizontal line denotes $U_E=2/3$.
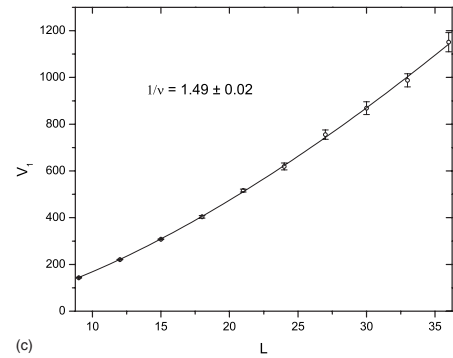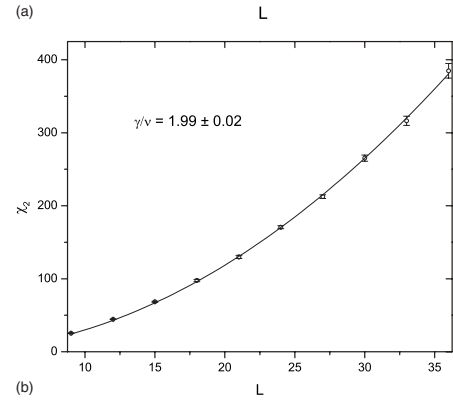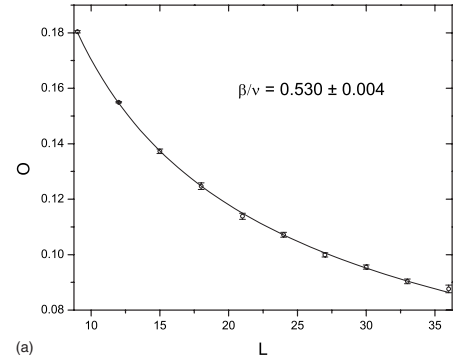

FIG. 4. Finite-size scaling of the order parameter O, susceptibility χ_2, and the first logarithmic derivative of the order parameter V_1 for case II.

TABLE II. Comparison of the critical temperature and critical exponents determined in this work with other MC studies.

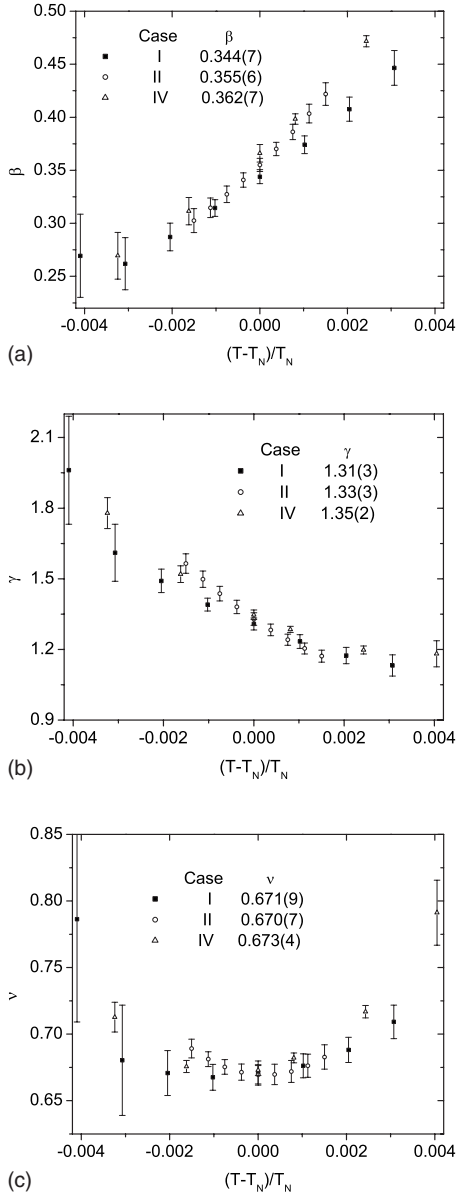|	T_N	β	γ	ν
I	2.926(3)	0.344(7)	1.31(3)	0.671(9)
Ref. 25	2.920(5)	0.311(4)	1.43(3)	0.685(3)
Ref. 12	2.9298(10)	0.341(4)	1.31(3)	0.662(9)
Ref. 14	2.88	0.19(1)	1.15(5)	
II	10.651(4)	0.355(6)	1.33(3)	0.670(7)
III	11.998(4)	0.358(5)	1.28(3)	0.677(3)
IV	7.406(6)	0.362(7)	1.35(2)	0.673(4)
Ref. 18	7.34(4)	0.21(1)	1.31(3)	0.70(3)
XY		0.345	1.316	0.671
Tricritical		1/4	1	1/2

(a)

(b)

(c)

FIG. 5. Values of the critical exponents β, γ, and ν for cases I, II, and IV, obtained for different choices of the critical temperature. Results for case III are qualitatively similar and have been omitted for clarity.
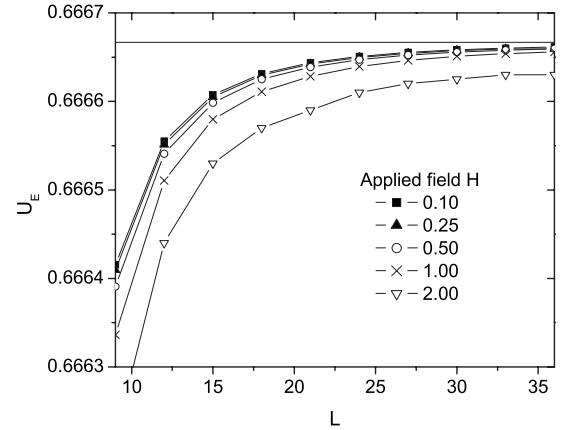

FIG. 6. Scaling of the energy cumulant U_E as a function of lattice size L is shown for several values of the applied field H. The horizontal line denotes $U_E = 2/3$.

nent ratios. Representative results using the exchange parameters in case II are shown in Fig. 4. Our data (not shown) indicate that the secondary order parameter O' is not relevant at T_N for $H=0$.

In Table II, the zero-field estimates of the critical temperatures and critical exponents determined in this work are compared with those obtained by other MC studies. For each case studied, our sets of critical exponents indicate 3D XY universality. This is in agreement with symmetry arguments as well as the MC results of Ref. 12 but contrast with the tricritical behavior seen in Refs. 14 and 18, where less intensive simulations were used.

In order to estimate errors due to the uncertainty in the critical temperature T_N, finite-size scaling analysis was performed at temperatures slightly above and below T_N. In Fig. 5, results are shown for the critical exponents β, γ, and ν versus the choice of critical temperature for cases I, II, and IV. We find that the cases with quasi-1D exchange interactions (cases II and IV) are more sensitive to the choice of critical temperature than the case with isotropic exchange coupling (case I). These results indicate that the critical temperature region is extremely narrow for the quasi-1D models, highlighting the need for care in the analysis and interpretation of both computational and experimental data for such systems.

IV. RESULTS AT NONZERO FIELD

The effects of a nonzero applied field were examined here for the quasi-1D case II only. This extends the work of Refs. 12 and 21 where isotropic exchange was assumed and where it is argued that the effect of an applied field is to change the symmetry to that of the three-state Potts model and hence the transition should be first order within mean-field theory. However, a more complicated phase diagram emerged as a result of these earlier MC simulations. The same number of MC steps as in the zero-field cases was used in the present study for equilibration and to calculate thermal averages. At field strengths $H=0.01$, 0.25, 0.50, and 1.00, simulation results for the energy cumulant shown in Fig. 6 extrapolate to

which U_M for lattice size L' intersects with the cumulants for $L=9$, 12, and 15. Linear fits are made using the results in the asymptotic region [i.e., $\ln^{-1}(L'/L) \lesssim 2.2$] and an estimate of the critical temperature T_N is obtained from the average value of the crossing points. The error $\pm \Delta T_N$ represents the standard deviation of these values.

The fourth-order energy cumulant U_E evaluated at T_N as a function of system size L for each of the four cases is shown in Fig. 3. The results extrapolate to $U_E^* = 0.666\,663(3)$ for $L \rightarrow \infty$ in all cases, as expected for a continuous phase transition where $U_E^* = 2/3$.

Finite-size scaling analysis at the critical temperature T_N of the various thermodynamic quantities $O \sim L^{-\beta/\nu}$, $\chi \sim L^{\gamma/\nu}$, and $V_1 \sim L^{1/\nu}$ was used to obtain estimates of critical expo-

TABLE III. Critical temperature and critical exponents for several points along the paramagnet phase boundary. The errors on the exponents are estimated from fits performed at $T=T_N\pm\Delta T_N$.

H	T_N	β	γ	ν
0	10.651(4)	0.35(2)	1.33(5)	0.670(7)
0.10	10.651(5)	0.31(3)	1.3(1)	0.63(1)
0.25	10.685(5)	0.28(3)	1.22(6)	0.56(1)
0.50	10.756(5)	0.27(4)	1.02(9)	0.50(2)
1.00	10.891(5)	0.27(7)	1.0(1)	0.48(4)

$U_E^* = 0.666\,663(3)$, suggesting that the phase transitions remain continuous at these lower field values. Results for the critical exponents at the five field strengths from $H=0$ to $H=1$ are shown in Table III. The error for the critical temperature is estimated from the scatter of the crossing points of the order-parameter cumulant data. The errors on the critical exponents are obtained from fits performed at $T=T_N\pm\Delta T_N$. For example, for $H=0.25$, the fits performed at $T=10.680$ yielded $\beta=0.26(1)$, $\gamma=1.28(4)$, and $\nu=0.56(1)$, whereas those at $T=10.690$ yielded $\beta=0.306(6)$, $\gamma=1.17(2)$, and $\nu=0.57(1)$. These results illustrate the sensitivity of the critical exponents with respect to the choice of critical temperature. The largest source of error on the critical exponents comes from the uncertainty in T_N. For small values of the applied field ($H=0.10$), the estimated values of the critical exponents β and ν are only slightly lower than the zero-field cases. At intermediate field values $H=0.50$ and $H=1.0$, the magnetic phase transition is characterized by a set of exponents that are consistent with tricritical mean-field values.

The finite-size scaling for a first-order phase transition has a different behavior and has been extensively tested in frustrated spin systems.[12,28] In Fig. 7, scaling of the fourth-order energy cumulant for the case $H=2.0$ evaluated at the critical temperature is plotted as a function of $1/N$, where N is the total number of spins. For a first-order phase transition, a linear scaling of the form $U_E=U_E^*+aN^{-1}$, with U_E^* different from $2/3$, is expected. The solid line is a linear fit to the data with $L\geq24$. For smaller lattice sizes, scaling with the volume is not expected and additional correction terms are im-
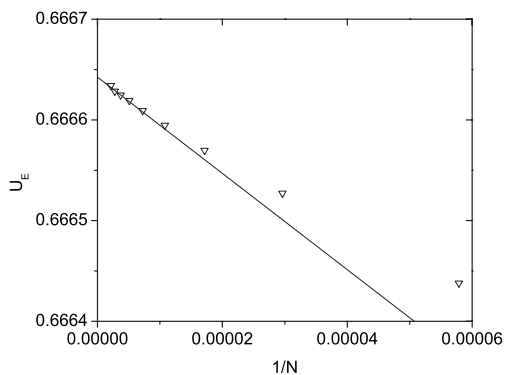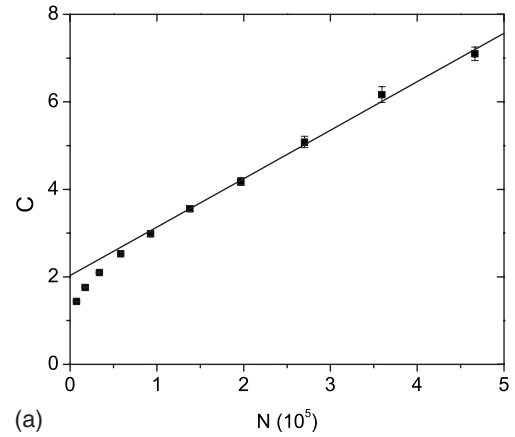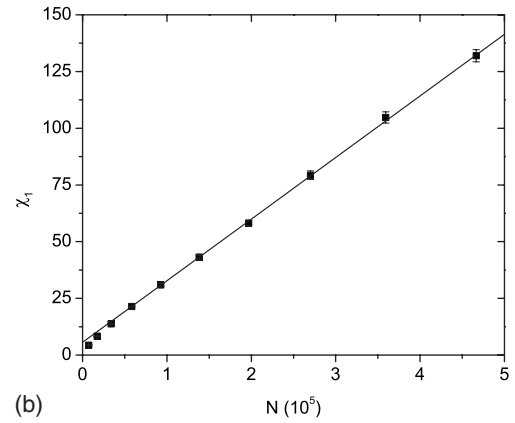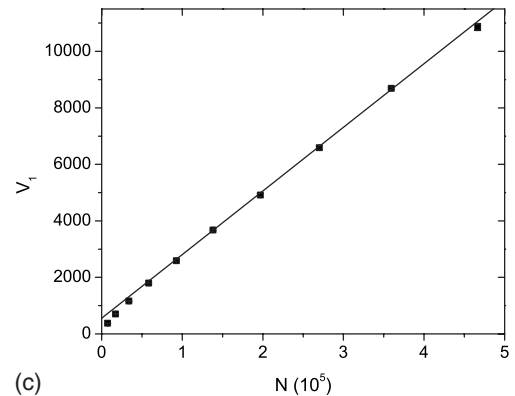

FIG. 7. Scaling of the energy cumulant U_E as a function of $1/N$ (where $N=10L^3$) for $H=2.0$. The solid line is a linear fit to the data with lattice sizes $L\geq24$.

FIG. 8. Scaling behavior of the specific heat C, susceptibility χ_1, and logarithmic derivative of the order parameter V_1 with the volume N. The solid lines are linear fits of the data with $L\geq24$.

portant. These considerations reveal a weak first-order phase transition with $U_E^*=0.666\,642(3)<2/3$. The asymptotic scaling of the specific heat C, susceptibility χ_1, and the logarithmic derivative of the order parameter V_1 with volume is shown in Fig. 8 for $H=2.0$. The linear scaling with volume N in these data confirms the first-order nature of the transition at this larger field strength.

V. CONCLUSIONS

The results of these extensive MC simulations using a combination of the CHB algorithm and histogram analysis

techniques serve to demonstrate the impact of quantum effects associated with the SRO in low-dimensional frustrated quantum spin systems on classical LRO critical behavior. This work serves to resolve long-standing questions regarding both experimental and previous modeling results on the critical properties of the quasi-1D ISTAF where both *XY* and tricritical behavior have been reported. Quantum effects due to SRO inherent in the quasi-1D $S=\frac{1}{2}$ compounds are emulated by the addition of a small applied field (which govern soliton dynamics in the ISTAF) and are shown here to induce a crossover from *XY* to tricritical, then first-order behavior. These results explain recent data on CsCoBr$_3$,[16] where the strength of the staggered field term had previously been es-

timated to be $H/J_0=0.05$,[9] consistent with our simulation results ($H=0.5$). Such effects have potential relevance in a wide variety of low-dimensional frustrated systems such as Cs$_2$CuCl$_4$ (Refs. [2], [4], and [5]) and especially Na$_{0.5}$CoO$_2$ where an unusual critical exponent of $\beta=0.28$ has been reported.[3]

[1] R. Moessner and A. P. Ramirez, Phys. Today **59** (2), 24 (2006).

[2] J. Alicea, O. I. Motrunich, and M. P. A. Fisher, Phys. Rev. Lett. **95**, 247203 (2005).

[3] G. Gašparović, R. A. Ott, J. H. Cho, F. C. Chou, Y. Chu, J. W. Lynn, and Y. S. Lee, Phys. Rev. Lett. **96**, 046403 (2006).

[4] W. Zheng, J. O. Fjaerestad, R. R. P. Singh, R. H. McKenzie, and R. Coldea, Phys. Rev. Lett. **96**, 057201 (2006).

[5] O. A. Starykh and L. Balents, Phys. Rev. Lett. **98**, 077205 (2007).

[6] M. F. Collins and O. A. Petrenko, Can. J. Phys. **75**, 605 (1997).

[7] *Frustrated Spin Systems*, edited by H. T. Diep (World Scientific, Singapore, 2004); B. Delamotte, D. Mouhanna, and M. Tissier, Phys. Rev. B **69**, 134413 (2004).

[8] H. B. Braun, J. Kulda, B. Roessli, D. Visser, K. W. Krämer, H.-U. Güdel, and P. Böni, Nat. Phys. **1**, 159 (2005).

[9] S. E. Nagler, W. J. L. Buyers, R. L. Armstrong, and B. Briat, Phys. Rev. B **27**, 1784 (1983); J. P. Goff, D. A. Tennant, and S. E. Nagler, *ibid.* **52**, 15992 (1995); H. Shiba, Y. Ueda, K. Okunishi, S. Kimura, and K. Kindo, J. Phys. Soc. Jpn. **72**, 2326 (2003).

[10] H. Kuroe, A. Oosawa, T. Sekine, Y. Nishiwaki, and T. Kato, J. Phys. Soc. Jpn. **76**, 043713 (2007).

[11] R. M. Morra, W. J. L. Buyers, R. L. Armstrong, and K. Hirakawa, Phys. Rev. B **38**, 543 (1988).

[12] M. L. Plumer and A. Mailhot, Physica A **222**, 437 (1995).

[13] D. Blankschtein, M. Ma, A. N. Berker, G. S. Grest, and C. M. Soukoulis, Phys. Rev. B **29**, 5250 (1984); A. N. Berker, G. S. Crest, C. M. Soukoulis, D. Blankschtein, and M. Ma, J. Appl. Phys. **55**, 2416 (1984).

[14] O. Heinonen and R. G. Petschek, Phys. Rev. B **40**, 9052 (1989).

[15] O. Koseki and F. Matsubara, J. Phys. Soc. Jpn. **69**, 1202 (2000).

[16] M. Mao, B. D. Gaulin, R. B. Rogge, and Z. Tun, Phys. Rev. B **66**, 184432 (2002).

[17] G. Quirion, T. Taylor, and M. Poirier, Phys. Rev. B **72**, 094403 (2005).

[18] O. Koseki and F. Matsubara, J. Phys. Soc. Jpn. **66**, 322 (1997).

[19] F. Matsubara, A. Sato, O. Koseki, and T. Shirakura, Phys. Rev. Lett. **78**, 3237 (1997).

[20] A. M. Ferrenberg and R. H. Swendsen, Phys. Rev. Lett. **61**, 2635 (1988).

[21] R. R. Netz and A. N. Berker, Phys. Rev. Lett. **66**, 377 (1991).

[22] M. L. Plumer and A. Mailhot, J. Phys.: Condens. Matter **9**, L165 (1997).

[23] G. Quirion, X. Han, M. L. Plumer, and M. Poirier, Phys. Rev. Lett. **97**, 077202 (2006).

[24] P. Peczak, A. M. Ferrenberg, and D. P. Landau, Phys. Rev. B **43**, 6087 (1991).

[25] A. Bunker, B. D. Gaulin, and C. Kallin, Phys. Rev. B **48**, 15861 (1993).

[26] M. L. Plumer, A. Mailhot, R. Ducharme, A. Caillé, and H. T. Diep, Phys. Rev. B **47**, 14312 (1993); M. L. Plumer and A. Mailhot, *ibid.* **52**, 1411 (1995).

[27] K. Binder, Z. Phys. B: Condens. Matter **43**, 119 (1981).

[28] D. Loison and K. D. Schotte, Eur. Phys. J. B **14**, 125 (2000).